Phase-field model of compressive and tensile fractures in ductile sandstone, calibrated by P wave velocity measurement and moment tensor inversion

Xu Li
School of Minerals and Energy Resources Engineering, University of New South Wales, Sydney, Australia

Guangyao Si
School of Minerals and Energy Resources Engineering, University of New South Wales, Sydney, Australia

Joung Oh
School of Minerals and Energy Resources Engineering, University of New South Wales, Sydney, Australia

Ismet Canbulat
School of Minerals and Energy Resources Engineering, University of New South Wales, Sydney, Australia

ABSTRACT: Recently, a novel approach (phase field damage model) enabled the simulation of compression and tension-induced cracks quasi-statically and captured crack propagation within the FEM (finite element method) framework. However, the application of the phase-field damage model is restricted by the calibration of the crack diffusion parameter, which cannot be directly measured. In this study, we proposed a new elastoplastic phase-field damage model, calibrated from the AE (Acoustic emission) moment tensor inversion and ultrasonic wave velocity measurement. The phase-field damage variable is determined from P wave velocity measurement and acoustic moment tensor inversion. Specular decomposition is performed on the damaged tensor to distinct tensile and compressive microcracks. The evolution between tensile and compressive phase-field damage variables is hence to be considered independently. The proposed model shows great consistency with the laboratory observations and the application of the proposed model in COMSOL software enables to capture the quasistatic propagation of both tensile and shear fractures.

Keywords: phase-field damage, seismicity, rock mechanics.

1 INTRODUCTION

The understanding of discontinuities is still an arduous task for rock mechanics, and the formation of geotechnical incidences (You et al. 2021; Li et al. 2022), akin to rock bursts, roof sagging and large tunnel deformation, may more or less relate to discontinuities. The discontinuities are, however, of different lengths and scales, ranging from several millimetre microcracks in laboratory tests to kilometres of underlying faults, which can induce high-energy earthquakes. Also, the propagation and coalescence of multiple discontinuities would generate a complex secondary stress field and complicate geotechnical hazard management. Hence, the simulation of microcracking behaviour numerically is difficult.

A novel and recent new approach to simulate the mechanical response of discontinuities is to use the phase-field damage method in FEM (Li et al. 2023). The application of the phase-field damage method provides another attitude to smear the discontinuous boundary into the phase damage field (You et al. 2021). The initiation, propagation, and coalescence of microcracks can be simulated

according to the multi-field coupling solver. This innovative approach avoids the requirement of any shape functions, compared with previous XFEM methods, but enables a more physical description regarding the profile of discontinuities (advantages compared to the DEM methods) (Li et al. 2023). The phase-field damage method has been introduced into different materials (e.g., rock and metal) and shows significant power in simulating discontinuities.

However, the application of the phase field damage model is still restricted by model calibration. In order to reflect the surface energy consumed to induce crack propagation, the profile of microcracks requires to be specified in the phase-field damage mode. The most important profile of microcracks is the crack width and critical fracture energy. The first parameter is critical fracture energy, indicating the energy consumed to generate the unit length of discontinuity. According to fracture mechanics, the critical fracture energy is related to mode I or mode II toughness and several ISRM suggested methods can be applied to measure the critical fracture energy (Hatheway 2009). The crack width represents the aperture of microcracks and also defines the diffusion width of the phase-field damage zone, which is hard to be directly measured. We notice that some studies only use the minimum size of the mesh as the crack width and some other studies may phenomenologically estimate this parameter from the rock UCS based on empirical equations (Fang et al. 2020). Since the crack width (length scale parameter) plays a dominant position in the propagation of cracks, the selection of the length scale parameter controls the entire stress-strain constitutive relationship of rock material. The value of the abovementioned length scale parameter requires to be carefully selected to obtain the best result.

Also, from fracture mechanics, the large deviation between tensile and shear cracks is proved in extensive pioneering research (Griffith 1921). The famous Griffith's model suggests that the compressive strength of rock material is eight times higher than the tensile strength. This observation indicates that the critical fracture energy consumed to generate per unit of compressive crack is much higher than the tensile crack. Then, the calibration of the phase-field damage model requires separating internal compressive and tensile cracks, which can be performed by an acoustic emission monitoring system. The focal mechanism of source events can be inversed via calibrated AE sensors.

In this study, we proposed a new approach to calibrate the parameters in the phase-field damage variable via ultrasonic wave velocity and moment tensor inversion of acoustic emission results. The moment tensor inversion separates tensile and compressive cracks inside rock samples, which assists to calibrate the length scale parameter and critical fracture energy for both tensile and shear cracks. The model is applied to COMSOL software, and the propagation of tensile and shear cracks can be observed separately.

2 METHODOLOGY

2.1 Application of moment tensor inversion in the microcracking damage theory

The relationship between the traditional damage variable and phase-field damage variable is stated in our previous study (Li et al. 2023), where the parameters in the phase-field damage model are for general cracks (the separation between tensile cracks and shear cracks is not specified). Based on a previous study, we attempt to determine the shear and tensile cracks and their damage effect independently (Horii and Nemat-Nasser 1983). The damage variable (D_{ij}) can be expressed by the profile of microcracks:

$$D_{ij} = \sum_{k=1,n} \frac{v_k}{V} (\vec{n}_k \otimes \vec{n}_k) \tag{1}$$

where, v_k is the volume of each microcrack and $\vec{n}_k$ is the normal vector for the k_{th} crack, and V is the volume of the rock specimen. D_{ij} is the anisotropic damage tensor determined by internal microcracks. Moment tensor inversion results can be applied to determine the profile (volume v_k and direction $\vec{n}_k$) of each microcrack.

$$M_{kk} = \Delta V(3\lambda + 2\mu)\vec{b} \times \vec{n} \tag{2}$$

where, ΔV is the volume change of each seismic incident and is related to v_k if cracking opening is observed ($\Delta V > 0$). λ and μ are Lamé constants and shear modulus of rock material. And $\vec{b} \times \vec{n}$ is the direction cosine between the rupture direction of microcracks. This can be calculated from the eigenvalue of the moment tensor:

$$\vec{b} \times \vec{n} = \frac{M_1 - 2M_2 + M_3}{M_1 - M_3} \tag{3}$$

where, M_1, M_2 and M_3 are the maximum, intermediate and minimum eigenvalue of a moment tensor. To separate the microcracks into tension and compression categories, we introduce a R variable:

$$R = \frac{tr(M)}{|tr(M)| + \sum|m_i^*|} \tag{4}$$

where, $tr(M)$ is the trace of the moment tensor and m_i^* is the eigenvalues of the deviatoric moment tensor. According to a previous study (Zhao et al. 2019), we assume $R > 30\%$ as tensile failure and $-30\% < R < 30\%$ as shear failure.

2.2 Laboratory introduction

In this study, triaxial tests are conducted in the UNSW geomechanics laboratory using the Multiphysics high-pressure high-temperature rock testing system. The ultrasonic wave measurement is performed every 5 seconds to monitor the P wave velocity change during the entire triaxial loading. The axial force is applied by a servo-control platen, where the displacement of the axial platen is set as a constant. The hydrostatic stress is applied by hydraulic oil controlled by a pump. An 8-channel integrated acoustic acquisition system from MISTRA with eight AE sensors to collect potential seismic waveforms. Eight acoustic emission sensors are applied to increase the accuracy of results. The waveform data are further imported into Insite software from ITASCA to perform moment tensor inversion. In moment tensor inversion, we delete seismic events received by less than eight sensors to increase the quality of our seismic data.

3 PHASE-FIELD DAMAGE MODEL

The thermodynamic framework is well described in previous studies by the authors' research team and extensive pioneering studies. Due to the page restriction, we only selectively introduce the thermodynamic framework of the phase-field damage model. Basically, the entire recoverable energy can be written as Helmholtz free energy (φ) with three components ($\varphi_e, \varphi_p, \varphi_f$) (You et al. 2021):

$$\varphi(\varepsilon, \varepsilon_p, d, \nabla d) = \varphi_e(\varepsilon, d) + \varphi_p(\varepsilon_p, d) + \varphi_f(d, \nabla d) \tag{5}$$

where, ε is the strain tensor and d is the phase-field damage variable. ∇d is the spatial gradient of the phase-field damage variable. $\varphi_e, \varphi_p, \varphi_f$ are elastic, plastic, and surface Helmholtz free energy respectively. Equation (5) is more likely to be an integrated energy considering both tensile and shear cracks. To separate the entire Helmholtz energy into tensile and shear components, some previous studies only separate the term of surface energy (φ_f) but do not decompose the phase-field damage variable (Bryant and Sun 2018). Even though the results coming from numerical simulation based on the abovementioned approach are convincing, there is still a research gap between the separation of tensile and shear cracks in their numerical model. Herein, this study aims to separate the phase-

field damage variable into its tensile and shear components (d^+ and d^-). And elastic and surface damage components in Helmholtz free energy are hence separated as:

$$\varphi_e(\varepsilon, d^+, d^-) = \frac{\lambda}{2}\left(g(d^+) + g(d^-)\right)tr(\varepsilon)^2 + g(d^-)\mu\sum_{a=1}^{3}(\varepsilon)^2 \tag{6}$$

Equation (6) has a robust physical meaning, indicating that the shear crack is induced from both hydrostatic and deviatoric parts of elastic Helmholtz free energy, and on the other hand, the tensile cracks only relate to the hydrostatic part of elastic Helmholtz free energy. For the surface energy of tensile and shear cracks, the energy is coming from a path integral along the propagation of the crack path. Hence, the expression of the surface Helmholtz free energy term is (You et al. 2021):

$$\varphi_f = \mathcal{G}_c^- \left(\frac{d^{-2}}{2l_-} + \frac{l^-}{2}\nabla d^- \cdot \nabla d^-\right) + \mathcal{G}_c^+ \left(\frac{d^{+2}}{2l_+} + \frac{l^+}{2}\nabla d^+ \cdot \nabla d^+\right) \tag{7}$$

where, $\mathcal{G}_c^-$ and $\mathcal{G}_c^+$ are the critical fracture energy for shear and tensile cracks respectively, whose determination procedures are regulated by ISRM suggested standards as well as pioneering studies from fracture mechanics. l^- and l^+ are length scale parameters for tensile and shear cracks, respectively, and the determination of such parameters requires assistance from damage mechanics, using ultrasonic wave velocity measurement and acoustic emission monitoring. The plastic part of the Helmholtz free energy is selected the same as in previous research (Li et al. 2023).

4 CALIBRATION OF THE LENGTH SCALE PARAMETER USING ULTRASONIC WAVE VELOCITY AND ACOUSTIC EMISSION

According to the previous study, parameters in the phase-field damage model can be related to the traditional damage model defined by ultrasonic wave velocity (Li et al. 2022).

$$\omega = 1 - \sqrt{\frac{v_p^2}{v_{p(max)}^2}} \tag{8}$$

where, v_p is the ultrasonic P wave velocity of rock samples and $v_{p(max)}$ is the maximum ultrasonic wave velocity of rock samples during the test. The relationship between the traditional damage variable (ω) and phase-field damage variable (d) has been stated in our previous studies, which enables us to obtain the phase-field damage variable from the change of ultrasonic wave velocity during the test.

In this study, we consider different damage variables, separating the tensile and shear effects. Hence, the traditional damage variable can be divided into the shear (ω^-) and tensile (ω^+) components. The shear and tensile components of the traditional damage variable can be back-calculated from the moment tensor inversion mentioned in Section 2.1.

$$\frac{d\omega^-}{d\omega^+} = \frac{D_{ij}^- n'_j n'_i}{D_{ij}^+ n'_j n'_i} \tag{9}$$

where, D_{ij}^- and D_{ij}^+ are damage tensors identified following Equations (1) and (4), n'_i and n'_j are direction vectors that define the direction of ultrasonic wave transmission. Hence, the parameter l_- and l_+ can then be calculated.

5 DETERMINATION OF THE LENGTH SCALE PARAMETER AND MODEL RESULTS

We took the 10MPa test as an example to evaluate the difference between the laboratory observation and analytical model results. Interestingly, the analytical model results (blue lines) and lab observations (red dots) show great consistency. After calibration, the length scale parameter is 8.39×10^{-6}m for tensile cracks and 8.37×10^{-7}m for shear cracks. The length scale parameter of shear cracks is significantly lower than tensile cracks, which coincides with our observations that shear cracks do not generate a high opening across the cracks. The propagation of cracks in notched samples is shown in Figure 2. We notice the propagation of both tensile and shear cracks, which indicates the robustness of our proposed model. The tensile cracks are manifested as vertical cracks, towards the top and bottom ends of the rock sample, whereas shear cracks are lateral cracks that horizontally propagate to the side of the rock sample. With the application of axial load, the length of both tensile and shear cracks increases, which indicates the crack propagation process is captured by the proposed model.

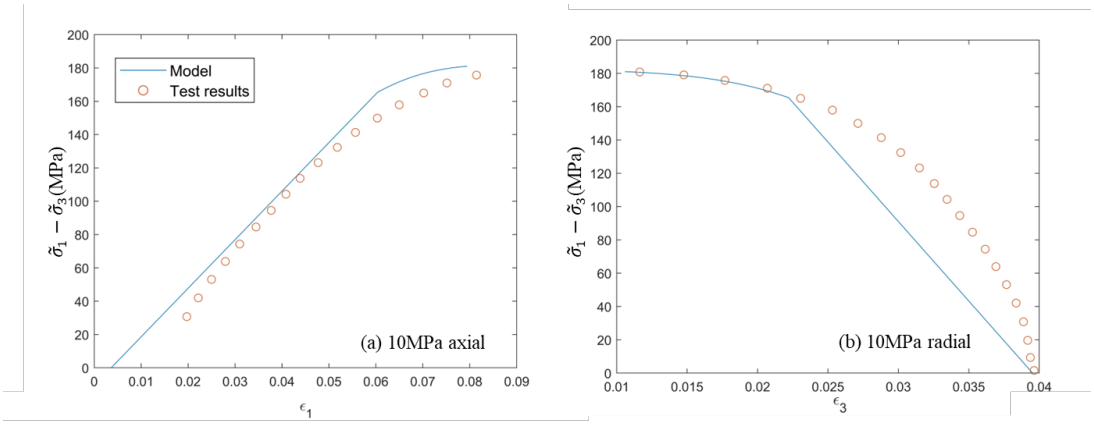

Figure 1. Comparison of the analytical model and laboratory test results in (a) axial and (b) radial direction under 10MPa.

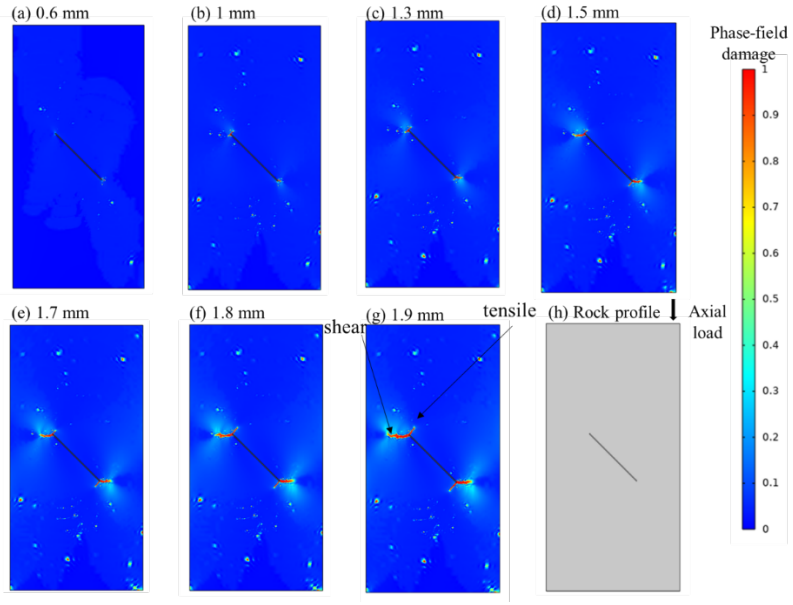

Figure 2. Tensile and shear crack propagation of a notched sample shown in (h) with the axial displacement of (a) 0.6 mm, (b) 1mm, (c) 1.3mm, (d) 1.5mm, (e) 1.7mm, (f) 1.8mm, and (g) 1.9mm.

6 CONCLUSION

This study provides new insight into considering tensile cracks and shear cracks separately in the phase-field damage model. Also, the calibration of the parameters of the proposed model is engaged via the assistance of ultrasonic wave velocity and acoustic emission monitoring systems. The damage variable is separated into tensile damage and shear damage, according to the focal mechanism of different microcracks. Then, the length scale parameter is calibrated based on the relationship between the damage variable and the phase-field damage variable. The model calibration indicates a close relationship between the proposed model and laboratory results. Then, the proposed model is imported into COMSOL software, and the propagation of tensile and shear cracks can be well-captured.

REFERENCES

Bryant EC, Sun W (2018) A mixed-mode phase field fracture model in anisotropic rocks with consistent kinematics. Computer Methods in Applied Mechanics and Engineering 342:561–584. https://doi.org/10.1016/j.cma.2018.08.008

Fang J, Wu C, Rabczuk T, et al (2020) Phase field fracture in elasto-plastic solids: a length-scale insensitive model for quasi-brittle materials. Computational Mechanics 66:931–961

Griffith AA (1921) VI. The phenomena of rupture and flow in solids. Philosophical transactions of the royal society of london Series A, containing papers of a mathematical or physical character 221:163–198

Hatheway AW (2009) The Complete ISRM Suggested Methods for Rock Characterization, Testing and Monitoring; 1974–2006. Environmental and Engineering Geoscience 15:47–48. https://doi.org/10.2113/gseegeosci.15.1.47

Horii H, Nemat-Nasser S (1983) Overall moduli of solids with microcracks: Load-induced anisotropy. Journal of the Mechanics and Physics of Solids 31:155–171. https://doi.org/10.1016/0022-5096(83)90048-0

Li X, Si G, Oh J, et al (2022) A pre-peak elastoplastic damage model of Gosford Sandstone based on acoustic emission and ultrasonic wave measurement. Rock Mech Rock Eng. https://doi.org/10.1007/s00603-022-02908-6

Li X, Si G, Wei C, et al (2023) Simulation of ductile fracture propagation using the elastoplastic phase-field damage method calibrated by ultrasonic wave velocity measurement. International Journal of Rock Mechanics and Mining Sciences 161:105296. https://doi.org/10.1016/j.ijrmms.2022.105296

You T, Waisman H, Chen W-Z, et al (2021) A novel micromechanics-enhanced phase-field model for frictional damage and fracture of quasi-brittle geomaterials. Computer Methods in Applied Mechanics and Engineering 385:114060. https://doi.org/10.1016/j.cma.2021.114060

Zhao Y, Yang T, Zhang P, et al (2019) Method for generating a discrete fracture network from microseismic data and its application in analyzing the permeability of rock masses: a case study. Rock Mech Rock Eng 52:3133–3155. https://doi.org/10.1007/s00603-018-1712-x